AD

EDGEWOOD ARSENAL
TECHNICAL REPORT

EATR 4636

MODIFICATIONS AND CHARACTERIZATION OF A LOW SPEED OPEN-CIRCUIT WIND TUNNEL

by

William A. Cooper

April 1972

DEPARTMENT OF THE ARMY
EDGEWOOD ARSENAL
Technical Support Directorate
Edgewood Arsenal, Maryland 21010

43

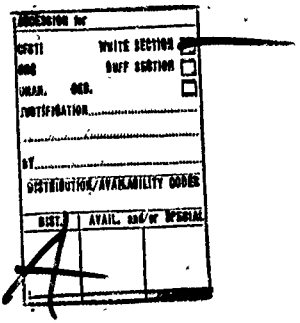

Distribution Statement

Approved for public release; distribution unlimited.

Disclaimer

The findings in this report are not to be construed as an official Department of the Army position unless so designated by other authorized documents.

Disposition

Destroy this report when no longer needed. Do not return it to the originator.

UNCLASSIFIED

Security Classification

DOCUMENT CONTROL DATA - R & D

(Security classification of title, body of abstract and indexing annotation must be entered when the overall report is classified)

1. ORIGINATING ACTIVITY (Corporate author) CO, Edgewood Arsenal ATTN: SMUEA-TS-TO Edgewood Arsenal, Maryland 21010	2a. REPORT SECURITY CLASSIFICATION UNCLASSIFIED 2b. GROUP NA

3. REPORT TITLE

MODIFICATIONS AND CHARACTERIZATION OF A LOW SPEED OPEN-CIRCUIT WIND TUNNEL

4. DESCRIPTIVE NOTES (Type of report and inclusive dates)

This work was started in August 1968 and completed in May 1971.

5. AUTHOR(S) (First name, middle initial, last name)

William A. Cooper

6. REPORT DATE	7a. TOTAL NO. OF PAGES	7b. NO. OF REFS
April 1972	49	13

8a. CONTRACT OR GRANT NO.	9a. ORIGINATOR'S REPORT NUMBER(S)
b. PROJECT NO.	4636
c. Task No. 1B062116A08402	9b. OTHER REPORT NO(S) (Any other numbers that may be assigned this report)
d.	

10. DISTRIBUTION STATEMENT

Approved for public release; distribution unlimited.

11. SUPPLEMENTARY NOTES	12. SPONSORING MILITARY ACTIVITY
	NA

13. ABSTRACT

The objective of this study was to improve the airflow characteristics of a low speed, open-circuit wind tunnel to allow its use for studying the impaction mechanisms of particles on collectors. In the work reported here, modifications to the settling chamber and transition section of the tunnel are described that resulted in an improved speed range (8.8 to 33 ft/sec) and an acceptable constant turbulence level (0.3%). Vertical and horizontal profiles of the longitudinal turbulent velocity component were obtained in the 30- by 24-inch working section with a constant temperature anemometer. It was found that the potential core extended approximately 10 inches in both dimensions.

14. KEYWORDS

Wind tunnel
Settling chamber
Damping screens
Filter paper
Turbulence
Hot-wire anemometer
Particle impaction
Spinning disk

DD FORM 1 NOV 68 1473 REPLACES DD FORM 1473, 1 JAN 64, WHICH IS OBSOLETE FOR ARMY USE.

UNCLASSIFIED

Security Classification

EDGEWOOD ARSENAL TECHNICAL REPORT

EATR 4636

MODIFICATIONS AND CHARACTERIZATION OF A LOW SPEED OPEN-CIRCUIT WIND TUNNEL

by

William A. Cooper

Test and Evaluation Division

April 1972

Task 1B062116A08402

DEPARTMENT OF THE ARMY
EDGEWOOD ARSENAL
Technical Support Directorate
Edgewood Arsenal, Maryland 21010

FOREWORD

The work described in this report was authorized under Task 1B062116A08402, Chemical Test and Assessment Technology. The wind tunnel was assembled in July and August 1968. The first modifications that significantly reduced the turbulence intensity and provided the range of windspeeds required for the particle impaction study were accomplished in March 1969. Additional modifications that reduced the turbulence intensity were performed in August 1970. The comprehensive proofing of the tunnel was done in April and May 1971. The experimental data are recorded in notebooks 8014, 8488, and 8565.

Acknowledgments

The author wishes to acknowledge the assistance of Wilbur Geho and Robert Burkmire.

DIGEST

The objective of this study was to improve the airflow characteristics of a low speed, open-circuit wind tunnel to allow its use for studying the impaction mechanisms of particles on collectors. In the work reported here, modifications to the settling chamber and transition section of the tunnel are described that resulted in an improved speed range (8.8 ft/sec to 33 ft/sec) and an acceptable constant turbulence level (0.3%). Vertical and horizontal profiles of the longitudinal turbulent velocity component were obtained in the 30- by 24-inch working section with a constant-temperature anemometer. It was found that the potential core extended approximately 10 inches in both dimensions.

CONTENTS

MODIFICATIONS AND CHARACTERIZATION OF A LOW SPEED OPEN-CIRCUIT WIND TUNNEL

I. INTRODUCTION.

An open-circuit aerosol wind tunnel was assembled to experimentally study the turbulent impaction phenomenon for a wide range of turbulent flow characteristics in order to formulate physical mathematical models for the turbulent impaction process. It was one of two open-circuit low speed wind tunnels that were received at the termination of contract DA 18-035-AMC-340(A), entitled "Investigation of Impaction Mechanisms of Particles on Collectors In Turbulent Flow." The large test section of this tunnel (24 inches wide, 30 inches high, and 72 inches long) was to be used to study the turbulent impaction phenomenon for a wider range of collector dimensions and particle sizes than those previously reported. The tunnel was designed to have a windspeed range of 5 to 45 ft/sec with a low background turbulence intensity and to accommodate collectors up to 15 inches in diameter with negligible wall interference.[1]

Preliminary hot-wire anemometer measurements of the streamwise velocity indicated that the windspeed range was only 10 to 24 ft/sec, with a nominal turbulence level of 5%. The poor performance was attributed to the entrance filter design and the method of controlling the windspeed. The urgency of the experimental impaction study and the lack of funds prevented changing the air induction system to a more suitable system employing a dc motor with variable speed control. Inexpensive and expedient modifications were necessitated to reduce the background turbulence level and to increase the windspeed range to allow better use of the tunnel for studying the impaction mechanisms of particles on collectors under potential flow conditions. The immediate objectives were to achieve a turbulence level less than or equal to 1% and a windspeed range up to 30 ft/sec. This was accomplished by simple modifications to the entrance filter housing and transition section. The subsequent addition of damping screens reduced the turbulence level to 0.3%. The modifications and results are described in this report. A detailed mapping of the longitudinal mean windspeed and turbulence intensity was performed using a constant-temperature hot-wire anemometer to proof the tunnel and to characterize the flow when an aerosol generator (spinning disk) was connected to the tunnel. In addition, a spectral distribution of the turbulent energy was obtained with high-pass filters and low-pass filters incorporated in the anemometer circuitry.

II. DESCRIPTION OF ORIGINAL AEROSOL WIND TUNNEL.

The general configuration and principal dimensions of the aerosol wind tunnel are shown in figure 1 (see the appendix). The tunnel is an open circuit draw-through type constructed of fiber glass. Room air enters the tunnel through the inlet filter housing, which serves to remove dirt particles from the air, to reduce the turbulence level, and to make the flow less susceptible to extraneous drafts in the room. The filter material is a low resistance filter paper* supported by glass fiber screen. The filter paper was selected on the basis of filtration efficiency, pressure drop, durability, and cost. The effectiveness of this material in suppressing room turbulence was demonstrated in a smaller wind tunnel used in previous experimental work.[2] All sides except the

[1] Torgeson, W. L. Litton Systems, Inc., Applied Science Division. Seventh Quarterly Report. Contract DA-18-035-AMC-340(A). Investigation of Impaction Mechanisms of Particles on Collectors in Turbulent Flow. March 1967. UNCLASSIFIED Report.

[2] Torgeson, W. L. Litton Systems, Inc., Applied Science Division. Ninth Quarterly Report. Contract DA-18-035-AMC-340(A). Investigations of Impaction Mechanisms of Particles on Collectors in Turbulent Flow. July 1967. UNCLASSIFIED Report.

*Developed by the Institute of Paper Chemistry, Appleton, Wisconsin, and designated IPC 1478 Pressure drop is 0.5 inch H_2O at face velocity of 78 fps.

back of the filter housing are covered with this filter paper. The back panel is plywood. The incoming filtered air passes through the convergence section, where it is accelerated when the cross section changes from a 6- by 6-foot square to a rectangular configuration 2.5 feet high and 2 feet wide in a distance of 5 feet. A uniform flow of air then passes in turn through the test section and the buffer section. Both of these sections are 6 feet long and rectangular with rounded corners and have slightly divergent walls to maintain a constant windspeed through the test section. Two Plexiglas windows are built into the sides of the test section for observing and placing probes, particle collectors, etc. The buffer section isolates the test section from the transition section where the rectangular cross-sectional shape of the tunnel is converted to the circular shape of the fan section. An adjustable louver is provided on each side of the transition section to regulate the airspeed. The induction system consists of a 7-vane Aerovent propeller fan driven by a 5 hp Westinghouse ac motor. The exiting air flows through a diffuser section having an area expansion factor of 1.5 and finally reenters the room after passing through an exit filter section, which prevents accumulation of aerosols in the room.

III. MODIFICATIONS OF THE AEROSOL WIND TUNNEL.

It is evident that some common and important features that are used in open circuit wind tunnels[3-7] to produce a steady and uniform flow with a low background turbulence intensity are missing. The tunnel does not have a flexible coupling to prevent the mechanical vibrations in the fan and diffuser from affecting the tunnel. The ac motor of the induction system is operated at a fixed rpm, and two bypass louvers are used to control the windspeed. A comparable dc motor with accurate speed control would have a speed range of at least 5 to 1.[7] Honeycomb straighteners and inlet screens[8] are commonly used to reduce swirl and turbulence in tunnels described in the literature. This tunnel has neither. It relies exclusively on the action of the filter paper. Another noteworthy departure from accepted practice is the unique entrance filter housing. Air is drawn into the tunnel through all sides of the entrance filter housing, but not through the back panel; that is, not in the direction of the mean flow.

The urgency of the turbulence impaction study and the lack of funds necessitated making expedient and inexpensive modifications to the existing tunnel to obtain windspeeds 30 ft/sec or greater and, more important, to reduce the background turbulence level to 1% or less. Conversion to the more commonly used dc motor with speed control or the purchase of precision-built honeycombs and inlet screens was not feasible. The methods employed and results obtained are described in the subsequent sections of this report.

The entrance filter is a single layer of IPC 1478 filter paper, which is composed of 70% cotton and scrim and 30% kronisol. It serves to remove dirt particles from the inlet air of the aerosol tunnel and to suppress the room turbulence. Its effectiveness in reducing the turbulence intensity was substantiated. The turbulence level in the test section was approximately 10 times greater without the filter paper. The airflow resistance of the IPC 1478 filter paper was determined

---

[3]Laufer, J. NACA TR-1174. The Structure of Turbulence in Fully Developed Pipe Flow. National Advisory Committee for Aeronautics. October 1952.

[4]Roshko, A. NACA TR-1191. On the Development of Turbulent Wakes From Vortex Streets. National Advisory Committee for Aeronautics. May 1952.

[5]Liepmann, H. W., and Fila, G. H. NACA TR-890. Investigation of Effects of Surface Temperature and Single Roughness Elements on Boundary Layer Transition. National Advisory Committee for Aeronautics. August 1946.

[6]Rose, W. G. Results of an Attempt to Generate a Homogeneous Turbulent Shear Flow. J. Fluid Mech. *25*, 97-120 (1966).

[7]Slater, C. Aero. Report 1218. National Physical Lab. Teddington (England). Low Speed Windtunnels for Special Purposes. December 1966. UNCLASSIFIED Report.

[8]Dryden, H. L., and Schubauer, G. B. The Use of Damping Screens for the Reduction of Wind-Tunnel Turbulence. J. Aero. Sci. *14*, 221-228 (1947).

to be twice that of eight layers of cheesecloth material. The latter material has been used in other low windspeed, low turbulence wind tunnels to filter the inlet air.[9,10] The greater airflow resistance results in a greater loss of kinetic or flow energy of the inlet air. However, considering the respective airflow resistances, the ruggedness of the materials, and the easy installation, the IPC 1478 filter paper was considered the better filtering material. To compensate for the energy loss, the entrance filter housing was enlarged, and the back plywood panel was replaced with the filter material. This also provided a more consistent flow. The inlet air was drawn into the tunnel axially as well as laterally. The new entrance filter housing had a filtering area of 228 sq ft, which was about three times the original design. The calculated inlet velocity of the air through the filter paper was reduced from 1.39 to 0.44 ft/sec, for a mean windspeed of 20 ft/sec.

The louver type bypass control in the transition section was replaced with a sliding door arrangement, and a third bypass door with a maximum opening of 200 sq in. was installed to compensate for the increase in the entrance filter area. Airspeeds lower than the control of the three bypass doors were obtained by inserting a constriction of IPC 1478 filter paper between the buffer and transition sections. Experimentally, it was determined that a single layer of IPC 1478 filter paper with and without a 168-sq in. open area would enable the airspeed to be decreased continuously to 5 ft/sec. A larger exit filter housing was designed and built to complement the larger entrance filter section. It also facilitates the replacement of the filter paper that is used to remove the aerosols from the airstream.

With these inexpensive and expeditious modifications, the windspeed range of the tunnel was increased, and the background turbulence level was reduced significantly. Further reduction of the turbulence level was achieved at some sacrifice of windspeed range by eliminating the inlet air that was drawn into the tunnel through the sides of the entrance filter and installing two damping screens in the inlet filter housing. These screens were expeditiously made from 36-inch wide standard 18-mesh glass fiber screening (17.5 meshes per inch and 0.014-inch fiber diameter). Two 6-foot lengths were joined together with limp nylon thread to form the 6- by 6-foot screen required. Care was taken to minimize the seam. The screens were inserted 2.5 and 5 feet from the entrance of the tunnel. This provides a 3-foot settling length between the second screen and the contraction section in which the small eddies generated by the screens can decay before entering the tunnel. The screens are in channels so that they can be removed for cleaning. A picture of the modified tunnel is shown in figure 2.

IV. EXPERIMENTATION.

A. Instrumentation.

A Datametrics type 1014 Barocel electronic manometer* with a type 511, 1-mm Hg, pressure sensor and a model 160-36 Dwyer static pitot tube** were used to determine the mean windspeeds of the tunnel and to calibrate the hot-wire anemometer used in measuring the background characteristics. The sensing element of the manometer is a high precision stable capacitive potentiometer encased in a gas-tight enclosure. A difference in total pressure within the enclosure produces a force that deflects a prestressed metal diaphragm and varies the relative capacitance of the diaphragm and fixed capacitor plates. The Barocel sensing element is electrically

[9] Corrsin, S. Decay of Turbulence Behind Three Similar Grids, Thesis for Degree of Aeronautical Engineer. Guggenheim Aeronautic Laboratory, California Institute of Technology. 1942.

[10] Asset, G., Gyrn, G. M., and Adams, E. A. CWL Special Publication 1-17. Windtunnel for Study of Aerosols in Turbulent Boundary Layer. July 1960. UNCLASSIFIED Report.

*Datametrics Inc., Waltham, Massachusetts.

**F. W. Dwyer Manufacturing Company, Inc., Michigan City, Indiana.

arranged in a 10-kc carrier-excited bridge so that a deflection of the diaphragm unbalances the bridge and produces a 10-kc voltage of amplitude proportional to the applied pressure.[11] An output voltage analog of the pressure difference was measured with a Tyco digital voltmeter* for increased reading accuracy. The manufacturer's stated specifications are: accuracy, 0.1 to 0.25 of reading; linearity to 0.05%; transient response at 760 mm Hg, 3 m sec.

Values of the streamwise (U-component) turbulence velocity were determined with a Thermo-Systems constant-temperature anemometer.** It incorporates a built-in linearizing module that compensates for the basic nonlinear relation between velocity and hot-wire voltage for constant temperature and constant density fluid. The manufacturer's specifications are: probe resistance measurement 0.25% accuracy; output noise level of anemometer less than 0.02% equivalent turbulence intensity or 70 μV RMS (root-mean-square) on a 0.0002-inch tungsten hot wire; linearity ±0.5% reading; output 0 to 10 volts for 0- to 30-ft/sec flow range. A sharp cutoff, 12dB/octave, 10-kHz low-pass filter was used to reduce noise pickup. Because the energy spectrum suggests negligible energy content for frequencies above 1000 Hz, this response should be adequate. The frequency response of this system using a conventional square wave test was 40 kHz at a mean windspeed of 20 ft/sec.

Probes were of the conventional single wire variety. The sensing element was a 0.00015-inch-diameter by 0.050-inch-long tungsten wire.

A Thermo-Systems model 1060** RMS voltmeter served to indicate the standard deviation of the longitudinal velocity. The True RMS meter utilizes accurate rectifier and square law functions to obtain a high crest factor and low frequency response characteristics that make it particularly applicable to measurements down to 0.1 Hz and averaging times up to 100 seconds. An averaging time constant of 10 seconds is used in this study as a satisfactory compromise between test time and frequency response. Overall frequency response of the instrument is 1 Hz to 500 kHz. Accuracy is ±1% full scale.

The RMS voltages and differential pressure measurements were digitized with Tyco model 404 digital voltmeter for increased reading accuracy. The manufacturer's specifications are: sensitivity, 100 μV; resolution, 0.01% FS; and accuracy, 0.02% reading ±1 digit.

Time averages were obtained with a Dymec integrating digital voltmeter, model 2401A,† and Precision time-it-timer.‡ Nominal integration time was 100 seconds.

The energy spectrum was conveniently measured with the sharp cutoff, 12dB/octave, high-low-pass filters incorporated in the model 1057 signal conditioner of the anemometer. The high-pass filter selections were: 2, 5, 10, 20, 50, 100, 200, 500, 1000, and 2000 Hz (-5%).

B. Test Procedure.

The building housing the open circuit wind tunnel was a converted warehouse that did not offer standardized control of the temperature and density of the air that flows through the tunnel. The temperature distribution in the room was not generally uniform and, in addition, the room was susceptible to drafts caused by space heater fans and outside wind gusts. The best

[11] Operations Manual. Type 1014 Barocel Electronic Manometer. p 5. Datametrics, Inc., Waltham, Massachusetts.

*Tyco Instrument Division, Waltham, Massachusetts.

**Thermo Systems, Inc., Saint Paul, Minnesota.

†Dymec, a division of Hewlett-Packard Company, Palo Alto, California.

‡Precision Scientific Company, Chicago, Illinois.

conditions for testing were found to occur on calm, cool, overcast days. The standard procedure was to operate the tunnel for about 30 minutes to achieve an "equilibrium" of the air temperature. The density of the air was determined from the barometric pressure, ambient temperature, and vapor pressure of the moist air using conversion tables. A calibration curve relating the differential pressure obtained with the electronic manometer and standard pitot tube to the mean windspeed was calculated from the reduced Bernouilli equation, i.e.,

$$V_0 = \sqrt{\frac{2(P_1 - P_0)}{\rho_{air}}} = \sqrt{\frac{2\rho_{Hg} g h}{\rho_{air}}}$$

where V, ρ, P, and h are conventional symbols for velocity, density, pressure, and height.

Calibration of the mean response of the hot-wire anemometer at 1.5 overheat ratio was carried out in the low turbulence potential core of the tunnel assuming the air temperature remained constant. Once this calibration had been accomplished, any changes in atmospheric pressure and vapor pressure during the testing time were ignored. A change in the mean air temperature was compensated for by adjusting the operating resistance of the hot-wire sensor to maintain a constant 1.5 overheat ratio. This method of compensation was especially useful on days when a temperature gradient was present in the test section. This condition usually occurred when the ambient temperature rose above 85°F.

C. Design of Experiment.

An Eulerian* description of the flow field in the test section is considered in this report. The method of time averaging is applied to the longitudinal velocity component at a fixed point. The instantaneous velocity is assumed to be made up of a fluctuating or irregular component of zero mean superimposed on a mean flow that is

$$U = \overline{U} + U'$$

where $\overline{U'} = 0$.

The intensity of turbulence or RMS value is defined as

$$U_{RMS} = \sqrt{\overline{(U')^2}}$$

The relative intensity or the turbulence level is defined as

$$\frac{\sqrt{\overline{(U')^2}}}{\overline{U}}$$

The temporal mean value, theoretically defined as

$$\overline{U} = \lim_{T \to \infty} \frac{1}{2T} \int_T^T U dt$$

was obtained by redefining $\overline{U}$, assuming the mean flow is independent of the origin of t

$$\overline{U} = \frac{1}{T} \int_0^T U(t + \tau)\, d\tau$$

*A system in which the time-varying properties of the fluid flow are assigned to points in space having fixed reference coordinates.

All data were obtained from a single tungsten hot-wire sensor positioned normally to the mean flow direction and a linearized constant temperature anemometer using an overheat ratio of 1.5. The time averages were obtained for a nominal integration time of 100 seconds. An average RMS value was calculated from 10 samples. If any abnormal readings occurred during the first set of measurements that appeared to be caused by extraneous disturbances (such as a draft) not actually characteristic of the flow, an additional 10 samples were taken and averaged. The average RMS values were kept in their electrical units to save computation time (3 ft/sec = 1 volt).

A more detailed description of turbulence was obtained by considering the distribution of energy among the turbulent eddies of different sizes. This idea is put into precise mathematical form by considering the distribution of energy with frequency (or wave number)

$$F(n) = 4\int_0^\infty R(\tau)\cos 2\pi n\tau d\tau$$

where $F(n)$, the spectral density function, is the cosine Fourier transform of the autocorrelation coefficient.[12]

$$R(\tau) = \frac{[U'(t)U'(t+\tau)]av}{\overline{(U')^2}}$$

The spectral distribution of turbulent energy is most conveniently measured by low-high-pass filters or bandpass filters and an RMS meter. In the present case, a high-pass filter incorporated with the Thermo-Systems anemometer was used; the results were obtained in the form used by Shaw, Lewkowicz, and Gostelow.[13]

$$f(n) = \frac{\left[\sqrt{\overline{(U')^2}}\right]_n^\infty}{\left[\sqrt{\overline{(U')^2}}\right]_0^\infty}$$

where $\left[\sqrt{\overline{(U')^2}}\right]_n^\infty$ is the energy in the spectrum from n frequency to ∞, and $\left[\sqrt{\overline{(U')^2}}\right]_0^\infty$ is the total energy in the spectrum. The maximum frequency was set at 10 kHz with low-pass filter. The lowest acceptable frequency was 1 Hz, the cutoff frequency determined by the time constant of the RMS meter. This overall frequency response was 1 Hz to 10 kHz.

V. TEST RESULTS AND DISCUSSION.

The entrance filter area was increased initially to 132 sq ft, and the original plywood panel on the rear of the filter section was kept intact. This arrangement increased the mean windspeed capability of the tunnel to 30 ft/sec. A third bypass door with a maximum opening of 200 sq in. allowed the windspeed to be reduced to 15 ft/sec. Figure 3 shows the relative turbulence intensity of the longitudinal velocity component measured along the central axis of the wind tunnel, 34 inches (downstream) from the entrance of the test section and 15 inches above the floor of the tunnel for this entrance filter configuration. The relative turbulence intensity increases from 4.5% at 15 ft/sec to 5.5% at 30 ft/sec.

[12] Condon, E. V., and Odishaw, H. Handbook of Physics. 3-30. McGraw-Hill Book Company, Inc., New York, New York. 1958.

[13] Shaw, R., Lewkowicz, A. K., and Gostelow, J. P. The University of Liverpool ULME/B.7. Measurements of Turbulence in the Liverpool University Turbomachinery Windtunnels and Compressor. September 1964.

The solid panel on the rear of the tunnel was then replaced with IPC 1478 filter paper, and an additional filter section was added providing 228 sq ft of filter area. The windspeed range of the tunnel was determined to be 17.5 to 40 ft/sec. Lower windspeeds were obtained by inserting a constriction of IPC 1478 filter paper between the buffer section and the transition section. A single layer of IPC 1478 filter paper with a 12- by 14-inch opening in conjunction with the bypass doors provided a nominal windspeed range of 7 to 15 ft/sec. A single layer of filter paper without any opening gave a windspeed range of 5 to 8 ft/sec. Figure 3 shows the relative turbulence intensity of the tunnel as a function of the windspeed for this entrance filter configuration. It is evident that inserting a constriction to reduce the windspeed has the adverse effect of increasing the intensity of the turbulence.

To reduce the turbulence intensity further, two damping screens were inserted in the entrance filter housing, and the filters in the sides of the housing were replaced so that all the inlet air entered the tunnel in the direction of the mean flow. The reduction in filter area reduced the maximum windspeed range of the tunnel to 33 ft/sec and offered a range of 8.8 to 33 ft/sec without the use of any constriction. The mean windspeed was reduced to 5 ft/sec by an IPC 1478 filter paper constriction with a 12- by 12-inch opening. The relative turbulence intensity for this configuration is also shown in figure 3 for comparison with previous conditions. A summary of the flow characteristics for the various configurations is given in the table.

Vertical and horizontal profiles of the mean and turbulence intensity of the longitudinal velocity, shown in figures 4 through 7, were used as a proof of the modified wind tunnel. The potential core at the 55-inch streamwise position had a uniform turbulence level of 0.3% and a width and height of 10 inches.

The spectral distribution of the turbulent energy of the longitudinal velocity component is shown in figure 8. It is evident that most of the energy is contained in frequencies less than 1000 Hz.

Because the tunnel was designed for investigating the impaction mechanisms of particles on collectors, the 2-inch spinning disk aerosol generator that will be used in the impaction study was connected to the tunnel, and a characterization of the flow of the complete system was made. The profiles are shown in figures 9 through 18. Examination of these profiles shows the presence of a noticeable peak in the turbulence intensity that corresponds in location to the center of the 8-inch-diameter connecting tube. The profiles become more and more flat with increasing streamwise distance. The uniform size of the potential core throughout the test section indicates that the divergence of the walls is effective in suppressing boundary layer growth.

Table. Summary of Flow Characteristics for Different Settling Chamber Configurations

Entrance filter area		Range	Turbulence level
Back panel	Side panels		
sq ft		*ft/sec*	*%*
0	72	10-24	5
0	132	15[a]-30	5
36	192	17.5[a]-40	1
36	0	8.8[a]-33	0.3[b]

[a]Bypass area of 600 sq in. available.

[b]Entrance housing contains two 18-mesh damping screens.

A constriction of IPC 1478 filter paper inserted between the buffer and transition sections was used to reduce the windspeed range of the tunnel from 10 to 5 ft/sec. The horizontal profiles of the mean and turbulence intensity with the aerosol generator connected to the tunnel are shown in figures 19 through 22. The peaks in the turbulence intensity that were particularly noticeable at the 4-inch streamwise position have been attenuated by the addition of the constriction. However, the turbulence level of the potential core was increased significantly and was not independent of the mean windspeed. The turbulence level at 10 ft/sec was 0.6% and increased to 1.3% at 5 ft/sec.

Several abnormal profiles were obtained during the proofing and characterization that serve to emphasize the need to prefilter the inlet air. The results are shown in figures 23 through 27. In figures 23 through 25, the prefilter on the spinning disk assembly that is used to remove dirt particles from the intake air was not used. Thus, unfiltered air was drawn through the aerosol disperser and into the tunnel. In figures 26 and 27, the nonuniformity was a result of a leak in the entrance filter housing.

VI. CONCLUSIONS.

It was found that the configuration of the entrance filter housing of the aerosol wind tunnel significantly affects the flow characteristics in the working section.

With a single layer of filter paper placed across the entrance of the tunnel and two inlet screens inserted in the entrance filter housing, turbulence levels measured fall within the range of turbulence levels (0.40%, 0.29%, and 0.30%) quoted by Shaw, Lewkowicz, and Gastelow[1,3] for the three tunnels at the University of Liverpool, but are high in relation to the values of some other low speed, open-circuit wind tunnels. Roshko[4] quoted a free stream turbulence level of 0.03%, Rose[6] quoted a value of 0.05%, and Liepmann and Fila[5] quoted a value of 0.0005%.

The free stream turbulence level of the modified tunnel is 0.3%. The speed range is 8.8 to 33 ft/sec.

The potential core or region of uniform intensity is at least 10 inches wide and 10 inches high throughout the test section of the tunnel.

A constriction of IPC 1478 filter paper placed downstream of the test section reduces the mean windspeed to 5 ft/sec, but it increases the turbulence level of the airstream from 0.6% at 10 ft/sec to 1.3% at 5 ft/sec.

LITERATURE CITED

1. Torgeson, W. L. Litton Systems, Inc. Applied Science Division. Seventh Quarterly Report. Contract DA-18-035-AMC-340(A). Investigation of Impaction Mechanisms of Particles on Collectors in Turbulent Flow. March 1967. UNCLASSIFIED Report.

2. Torgeson, W. L. Litton Systems, Inc. Applied Science Division. Ninth Quarterly Report. Contract DA-18-035-AMC-340(A). Investigations of Impaction Mechanisms of Particles on Collectors in Turbulent Flow. July 1967. UNCLASSIFIED Report.

3. Laufer, J. NACA TR-1174. The Structure of Turbulence in Fully Developed Pipe Flow. National Advisory Committee for Aeronautics. October 1952.

4. Roshko, A. NACA TR-1191. On the Development of Turbulent Wakes From Vortex Streets. National Advisory Committee for Aeronautics. May 1952.

5. Liepmann, H. W., and Fila, G. H. NACA TR-890. Investigation of Effects of Surface Temperature and Single Roughness Elements on Boundary Layer Transition. National Advisory Committee for Aeronautics. August 1946.

6. Rose, W. G. Results of an Attempt to Generate a Homogeneous Turbulent Shear Flow. J. Fluid Mech. *25*, 97-120 (1966).

7. Slater, C. Aero. Report 1218. National Physical Lab. Teddington (England). Low Speed Windtunnels for Special Purposes. December 1966. UNCLASSIFIED Report.

8. Dryden, H. L., and Schubauer, G. B. The Use of Damping Screens for the Reduction of Wind-Tunnel Turbulence. J. Aero. Sci. *14*, 221-228 (1947).

9. Corrsin, S. Decay of Turbulence Behind Three Similar Grids. Thesis for Degree of Aeronautical Engineer. Guggenheim Aeronautic Laboratory, California Institute of Technology. 1942.

10. Asset, G., Gynn, G. M., and Adams, E. A. CWL Special Publication 1-17. Windtunnel for Study of Aerosols in Turbulent Boundary Layer. July 1960. UNCLASSIFIED Report.

11. Operations Manual. Type 1014 Barocel Electronic Manometer. p 5. Datametrics, Inc., Waltham, Massachusetts.

12. Condon, E. V., and Odishaw, H. Handbook of Physics. 3-30. McGraw-Hill Book Company, Inc., New York, New York. 1958.

13. Shaw, R., Lewkowicz, A. K., and Gostelow, J. P. The University of Liverpool ULME/B.7. Measurements of Turbulence in the Liverpool University Turbomachinery Windtunnels and Compressor. September 1964.

APPENDIX

FIGURES

LIST OF FIGURES

LIST OF FIGURES (Contd)

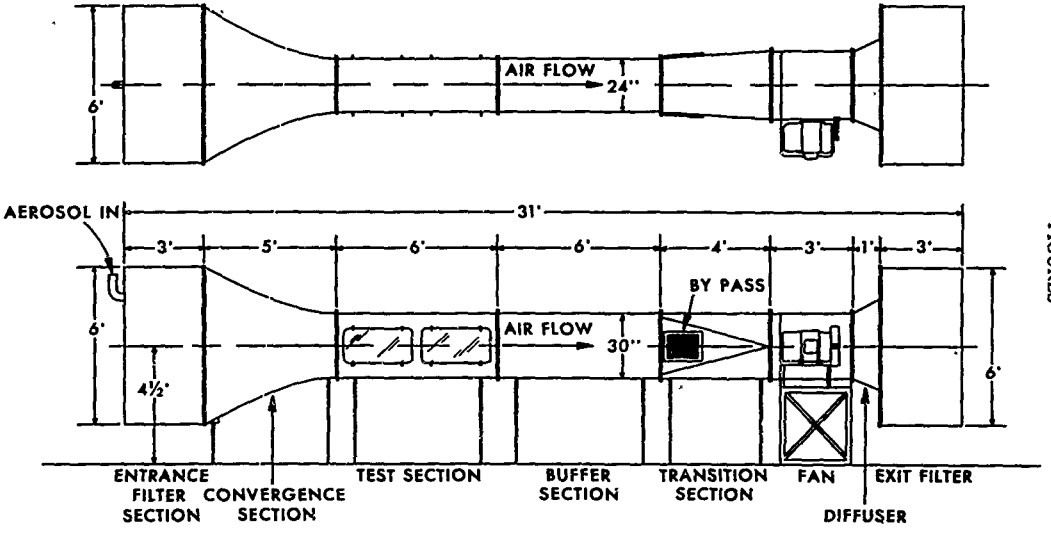

Figure A-1. Original Aerosol Wind Tunnel

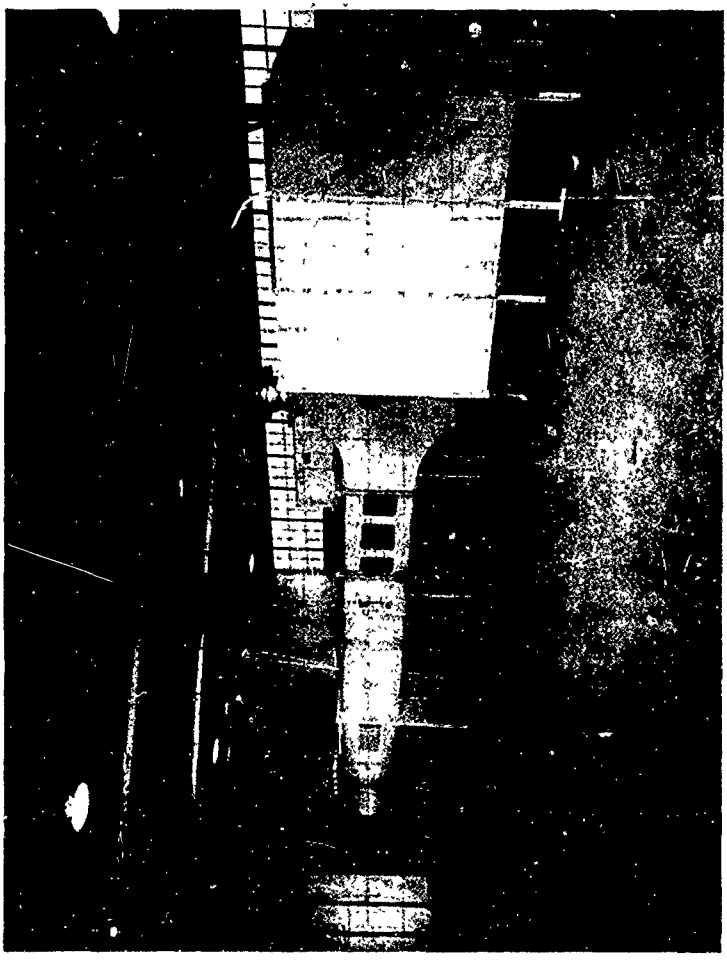

Figure A-2. Modified Aerosol Wind Tunnel and Facility

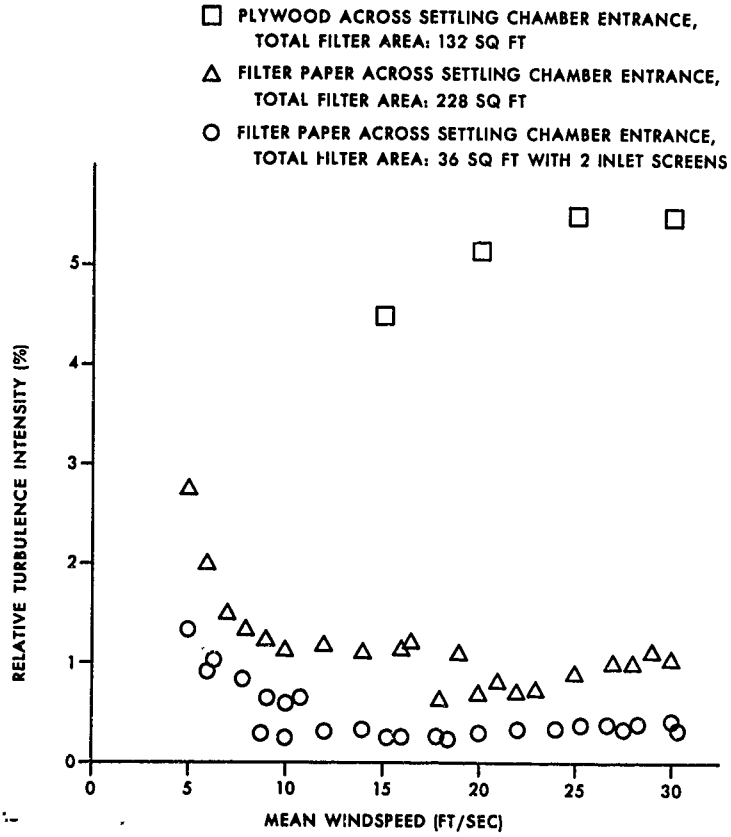

Figure A-3. Relative Turbulence Intensity for Three Settling Chamber Configurations

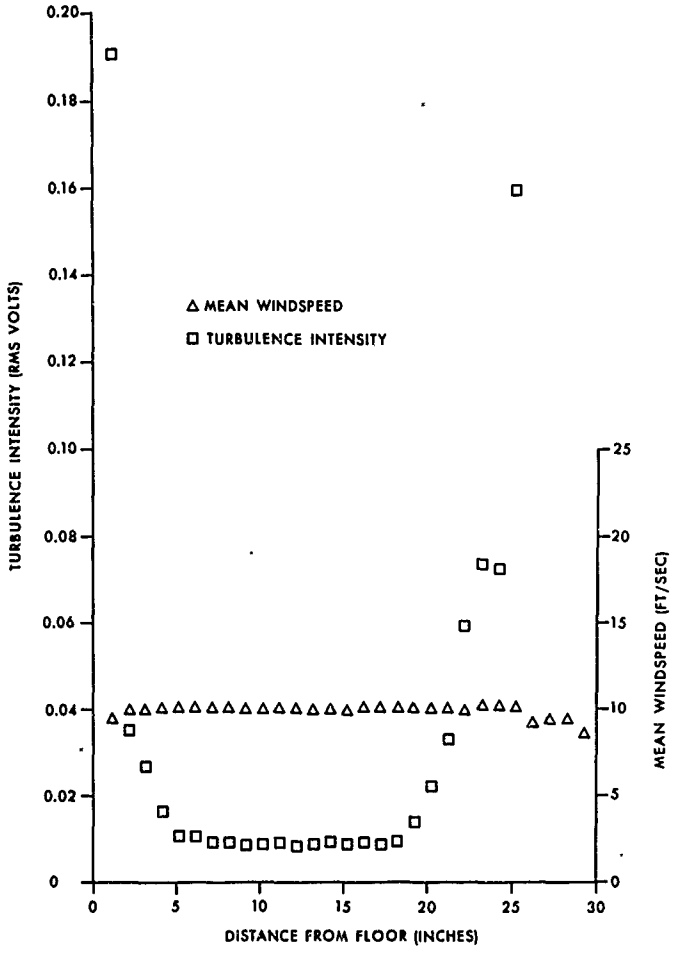

Figure A-4. Vertical Profile of the Longitudinal Velocity at Distance Downstream of 55 Inches

In figures 4 through 27, Δ = mean windspeed, and □ = turbulence intensity.

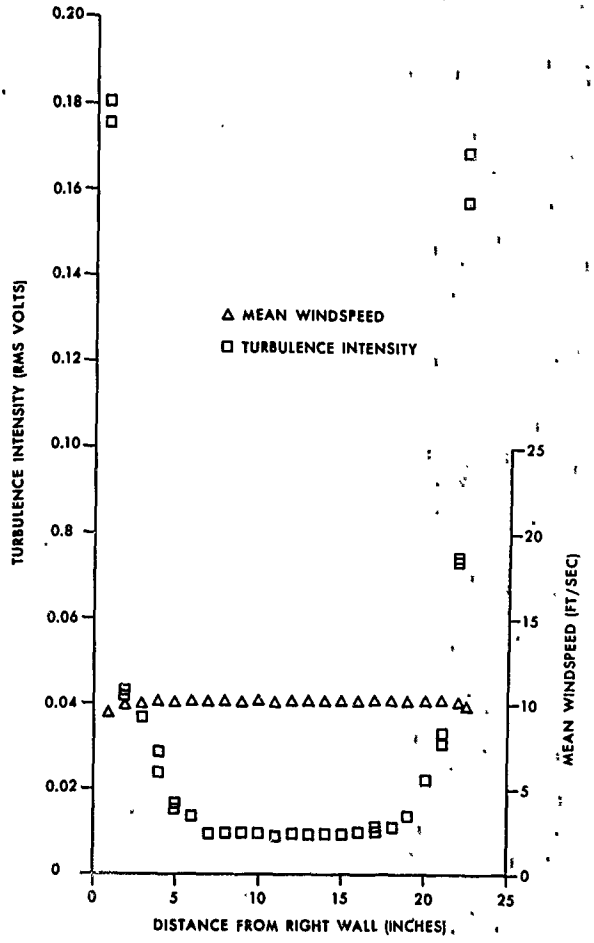

Figure A-5. Horizontal Profile of the Longitudinal Velocity at Distance Downstream of 55 Inches

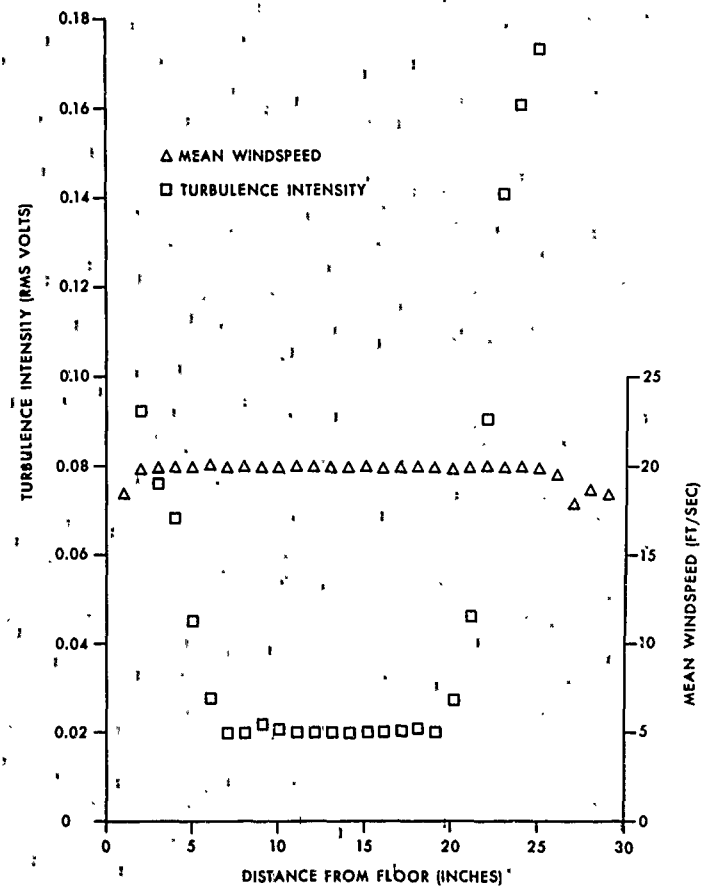

Figure A-6. Vertical Profile of the Longitudinal Velocity as Distance Downstream of 55 Inches

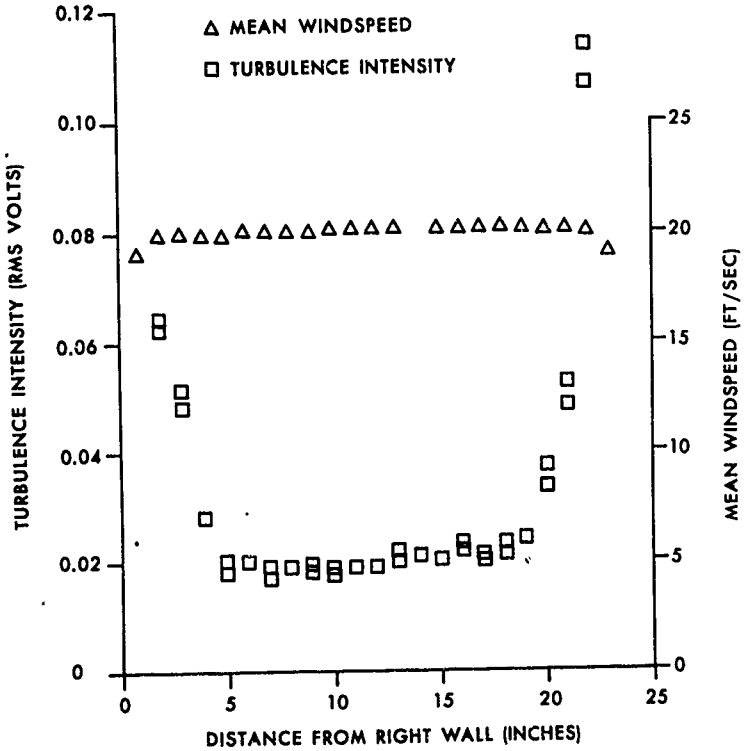

Figure A-7. Horizontal Profile of the Longitudinal Velocity at Distance Downstream of 55 Inches

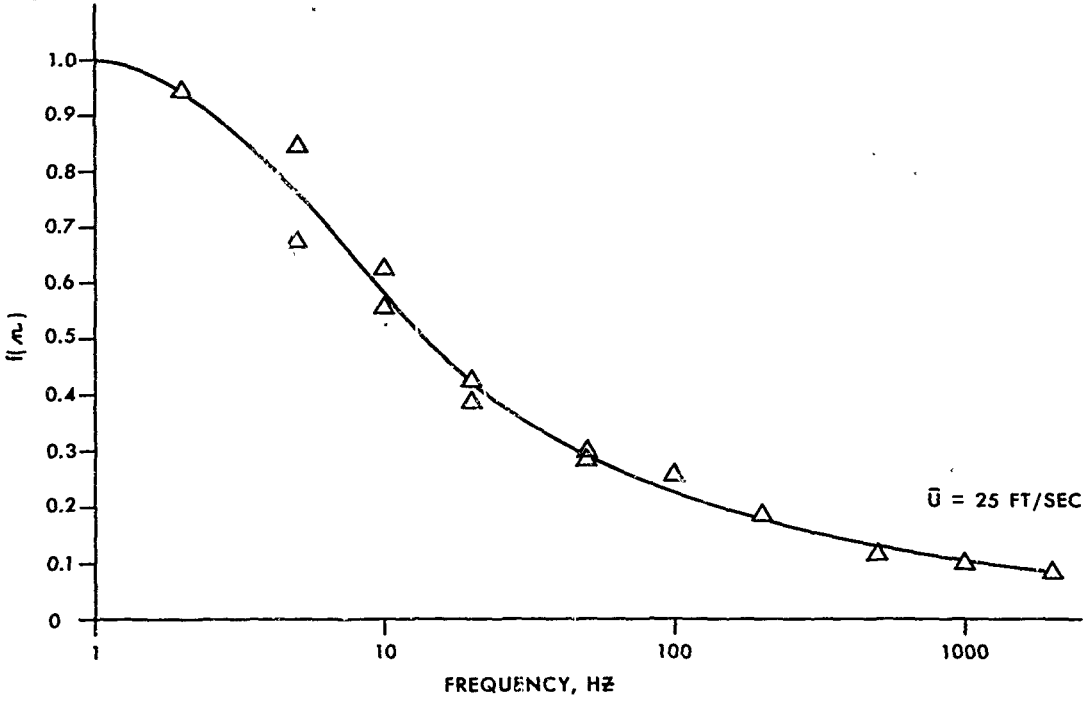

Figure A-8. Turbulence Spectrum of the Longitudinal Velocity

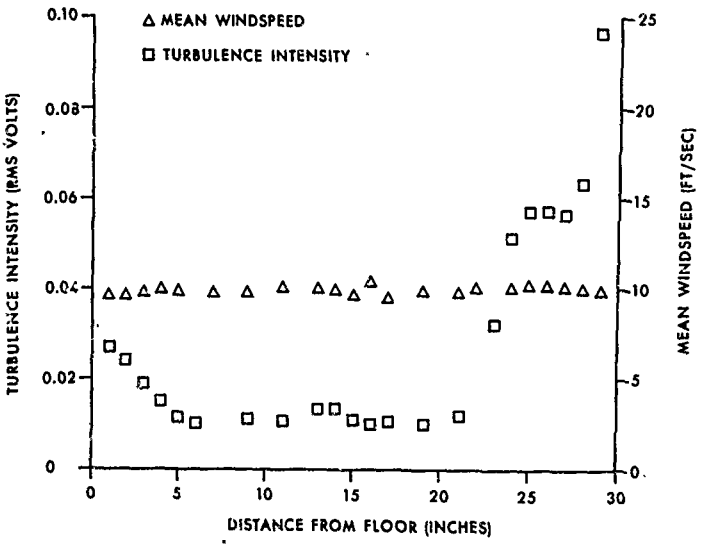

Figure A-9. Vertical Profile of the Longitudinal Velocity at Distance Downstream of 4 Inches (Aerosol Disperser Attached)

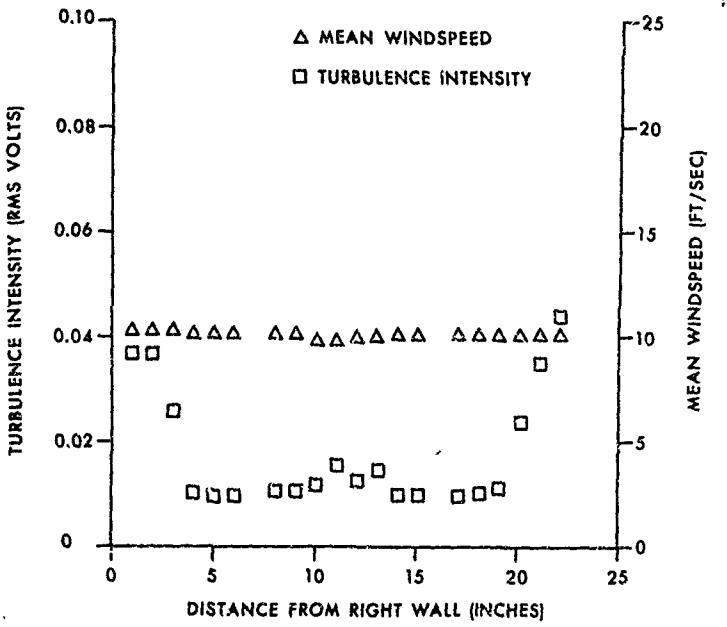

Figure A-10. Horizontal Profile of the Longitudinal Velocity at Distance Downstream of 4 Inches (Aerosol Disperser Attached)

Figure A-11. Vertical Profile of the Longitudinal Velocity at Distance Downstream of 4 Inches (Aerosol Disperser Attached)

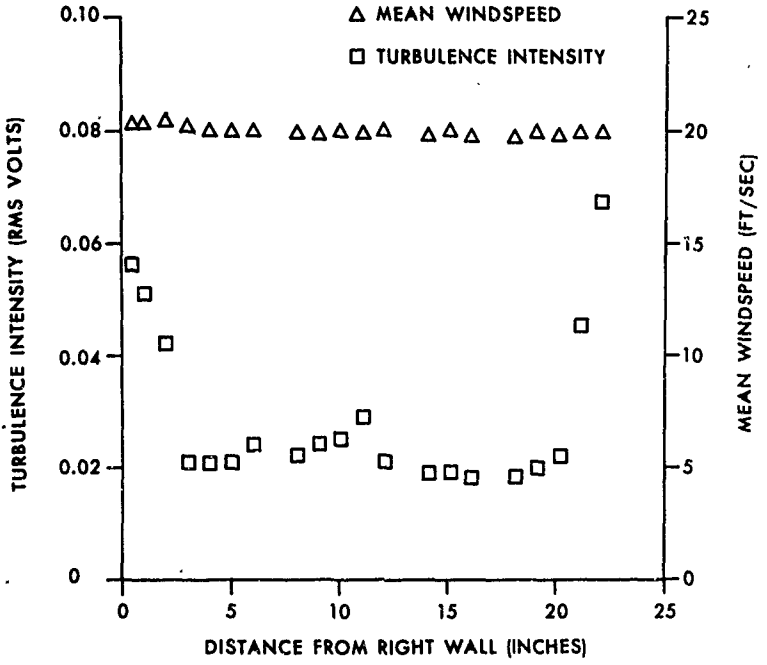

Figure A-12. Horizontal Profile of the Longitudinal Velocity at Distance Downstream of 4 Inches (Aerosol Disperser Attached)

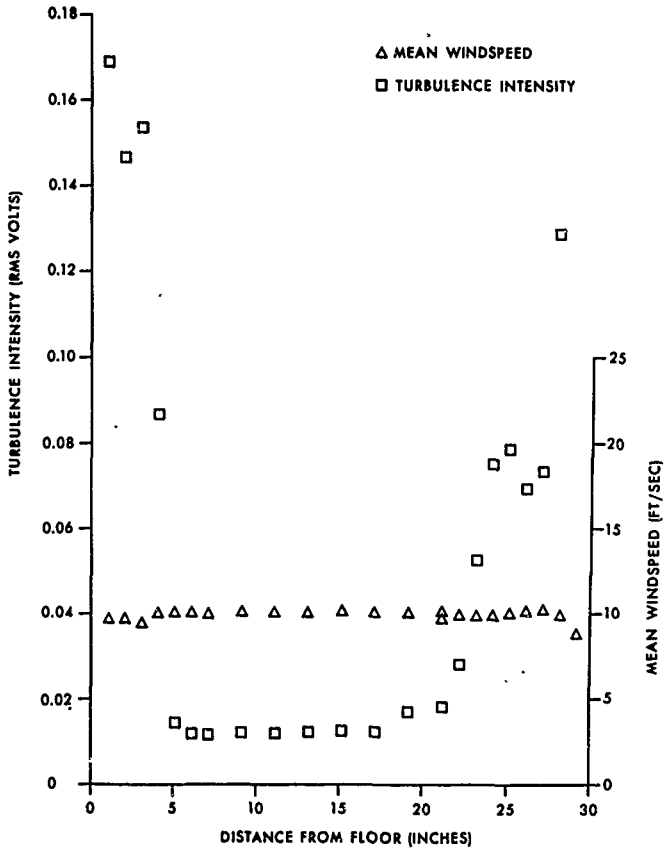

Figure A-13. Vertical Profile of the Longitudinal Velocity at Distance Downstream of 34 Inches (Aerosol Disperser Attached)

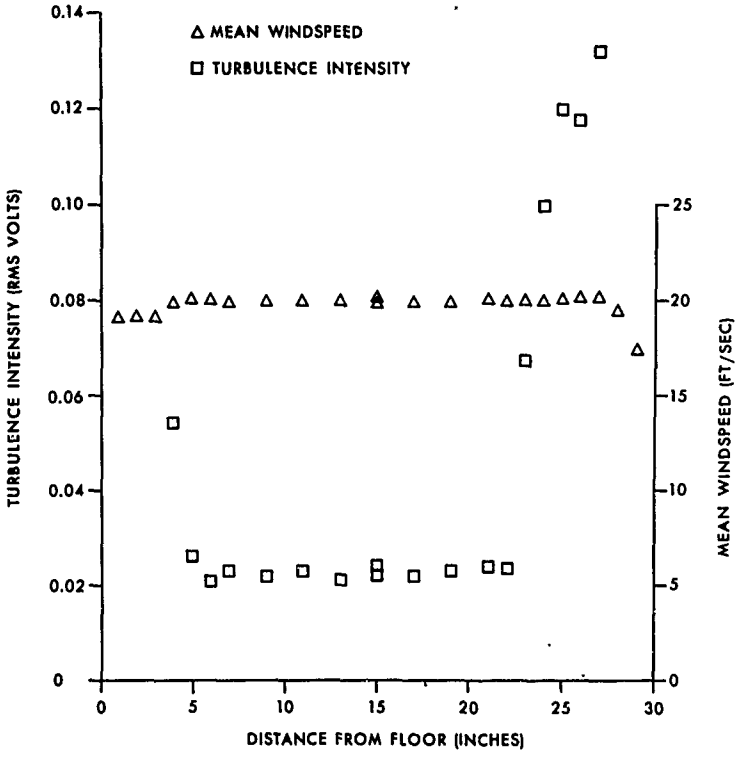

Figure A-14. Vertical Profile of the Longitudinal Velocity at Distance Downstream of 34 Inches (Aerosol Disperser Attached)

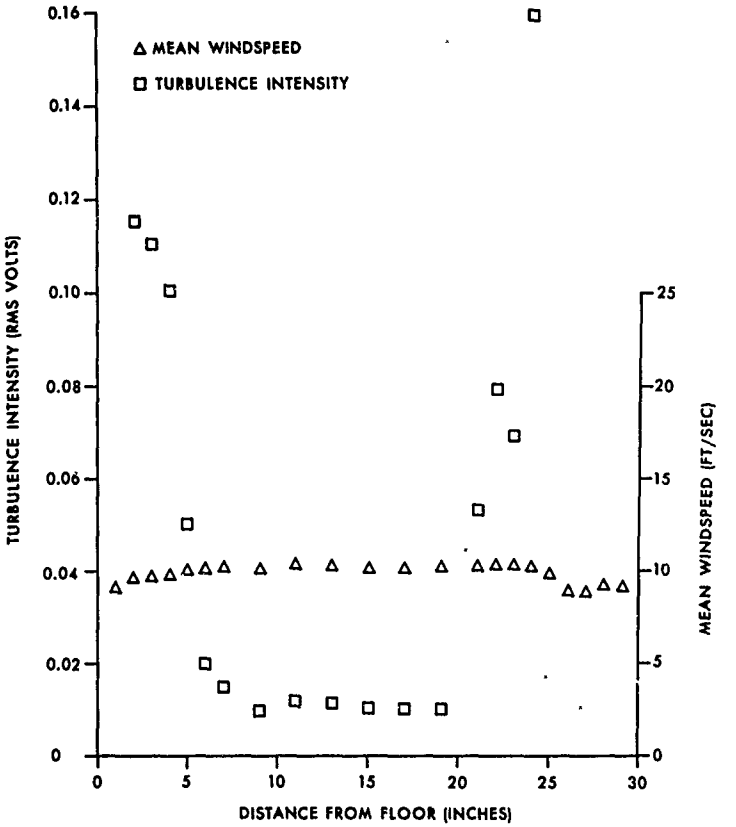

Figure A-15. Vertical Profile of the Longitudinal Velocity at Distance Downstream of 55 Inches (Aerosol Disperser Attached)

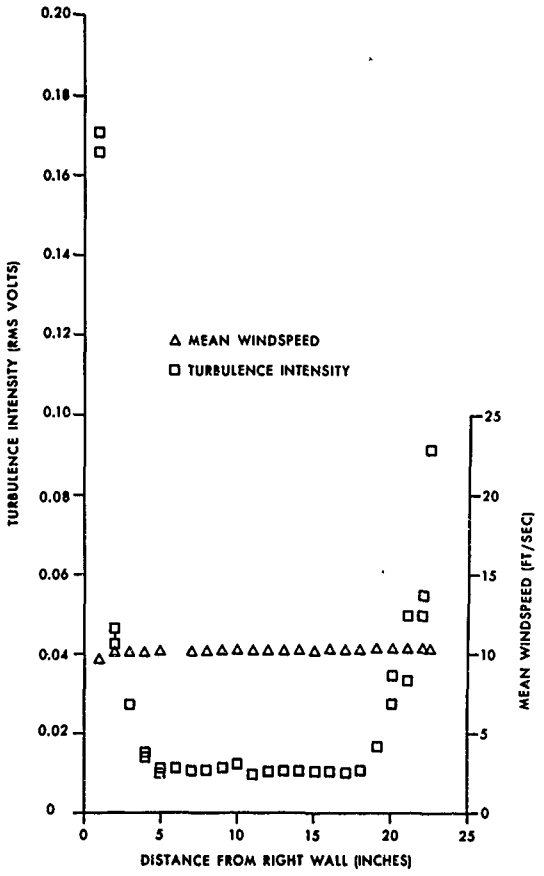

Figure A-16. Horizontal Profile of the Longitudinal Velocity at Distance Downstream of 55 Inches (Aerosol Disperser Attached)

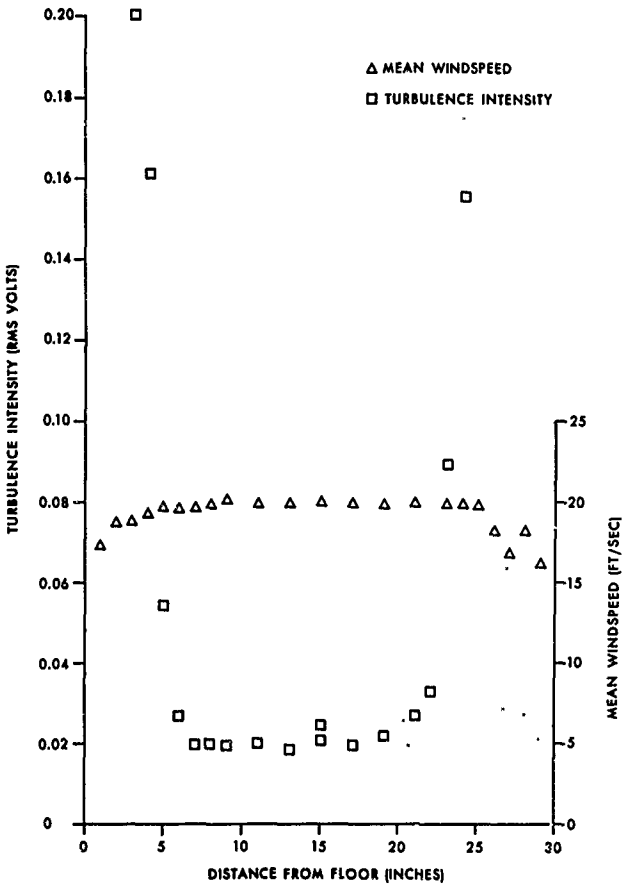

Figure A-17. Vertical Profile of the Longitudinal Velocity at Distance Downstream of 55 Inches (Aerosol Disperser Attached)

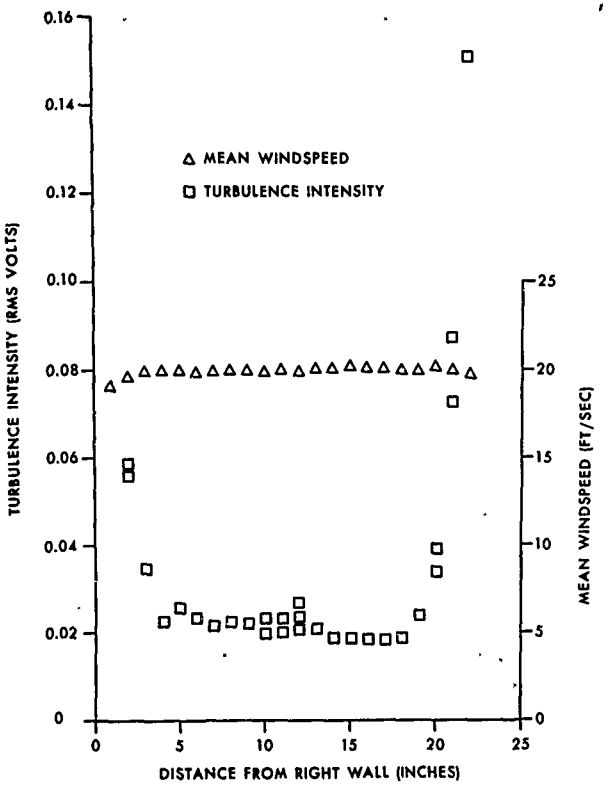

Figure A-18. Horizontal Profile of the Longitudinal Velocity at Distance Downstream of 55 Inches (Aerosol Disperser Attached)

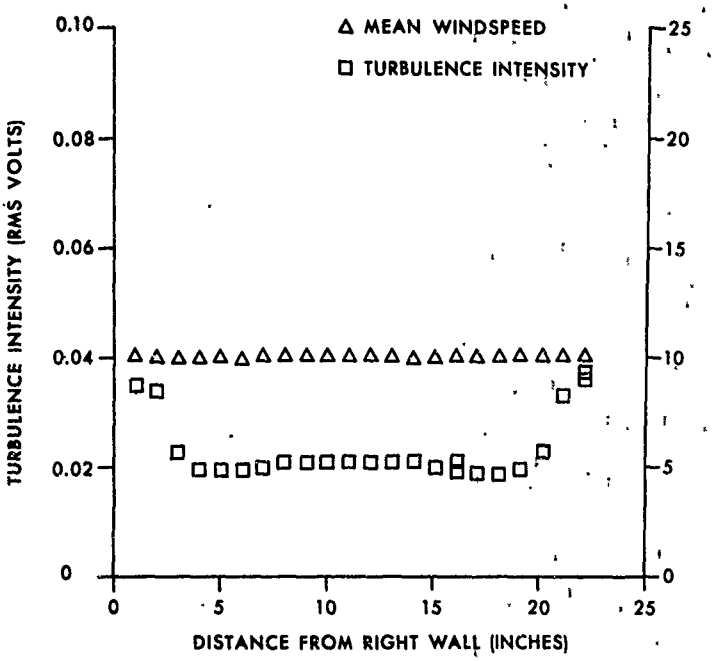

Figure A-19. Horizontal Profile of the Longitudinal Velocity at Distance Downstream of 4 Inches (Aerosol Disperser Attached and Constriction Included)

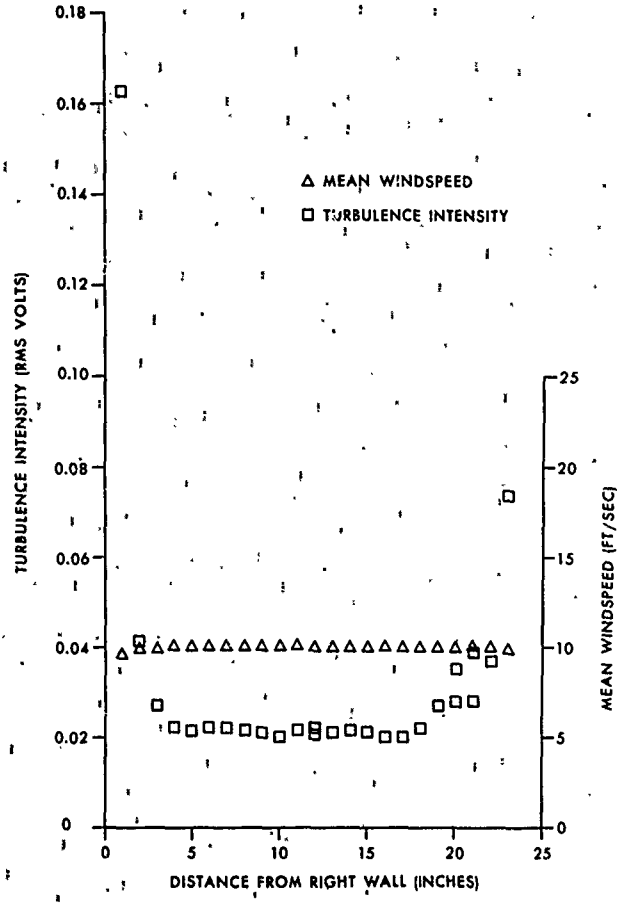

Figure A-20. Horizontal Profile of the Longitudinal Velocity at Distance Downstream of 55 Inches (Aerosol Disperser Attached and Constriction Included)

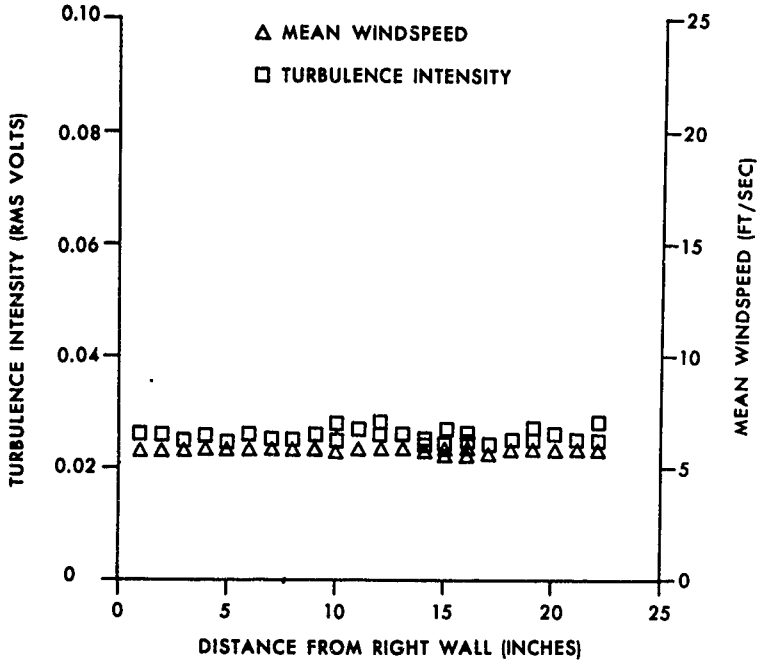

Figure A-21. Horizontal Profile of the Longitudinal Velocity at Distance Downstream of 4 Inches (Aerosol Disperser Attached and Constriction Included)

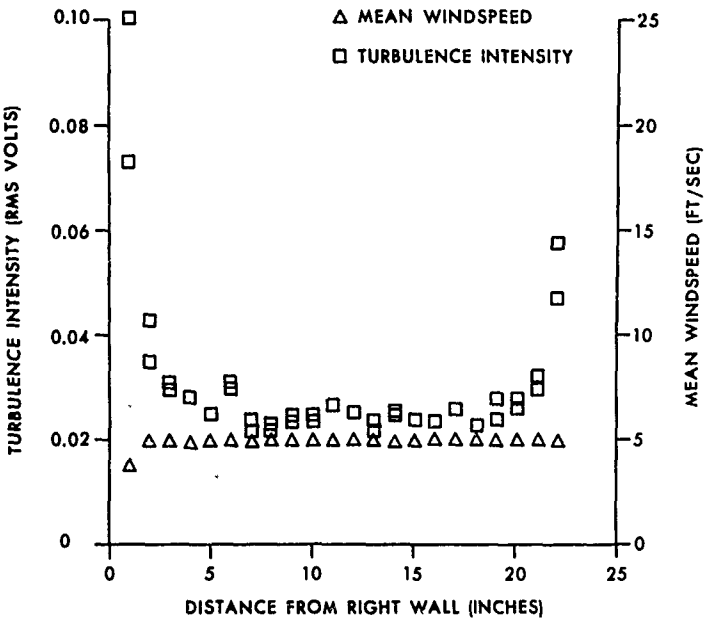

Figure A-22. Horizontal Profile of the Longitudinal Velocity at Distance Downstream of 55 Inches (Aerosol Disperser Attached and Constriction Included)

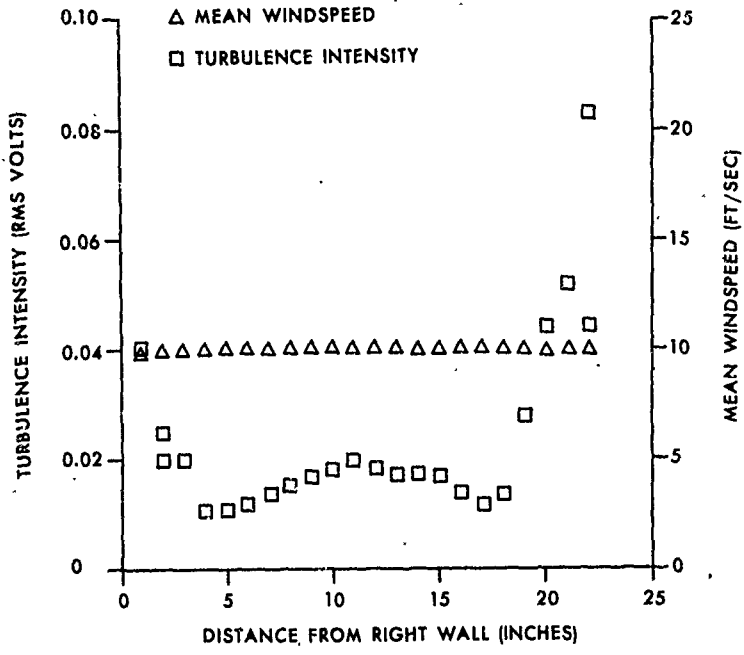

Figure A-23. Horizontal Profile of the Longitudinal Velocity at Distance Downstream of 34 Inches (Aerosol Disperser Attached)

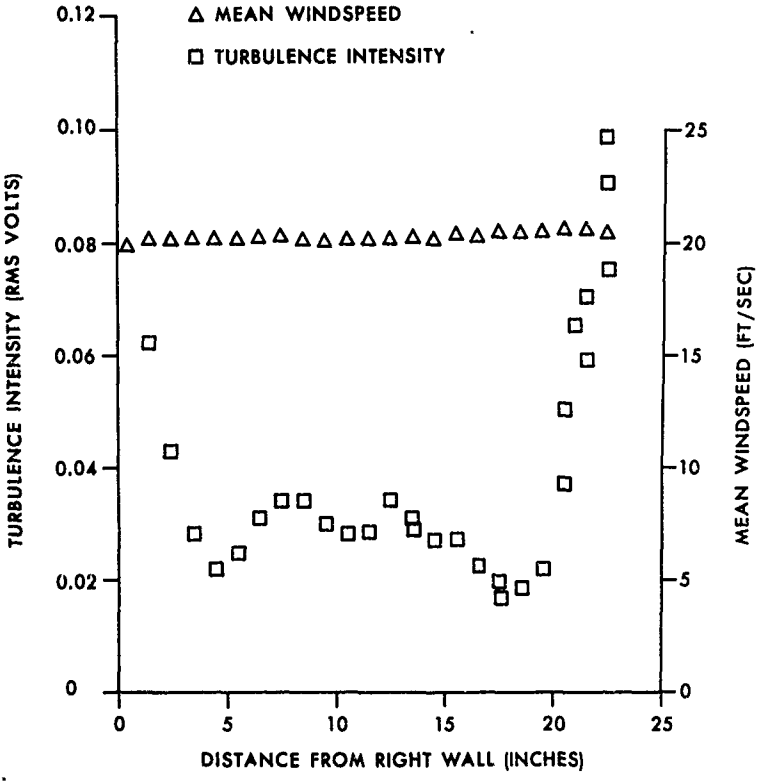

Figure A-24. Horizontal Profile of the Longitudinal Velocity at Distance Downstream of 34 Inches (Aerosol Disperser Attached)

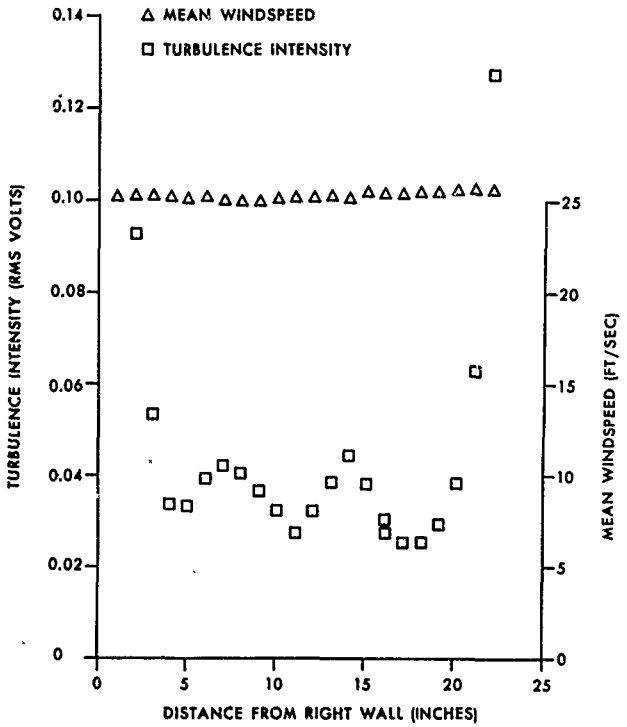

Figure A-25. Horizontal Profile of the Longitudinal Velocity at Distance Downstream of 34 Inches (Aerosol Disperser Attached)

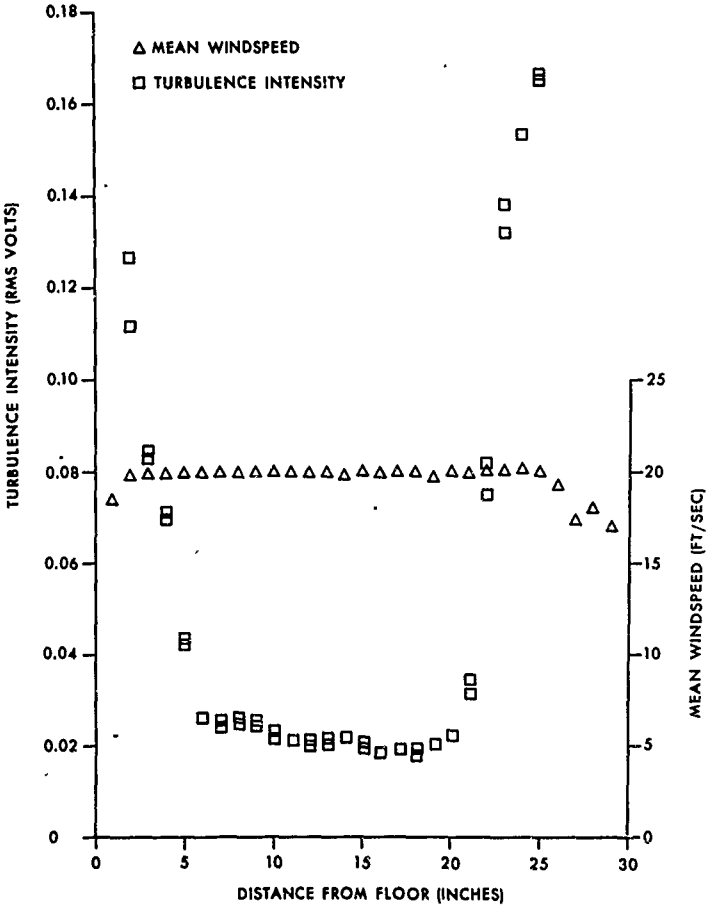

Figure A-26. Vertical Profile of the Longitudinal Velocity at Distance Downstream of 55 Inches With a Leak in the Entrance Filter

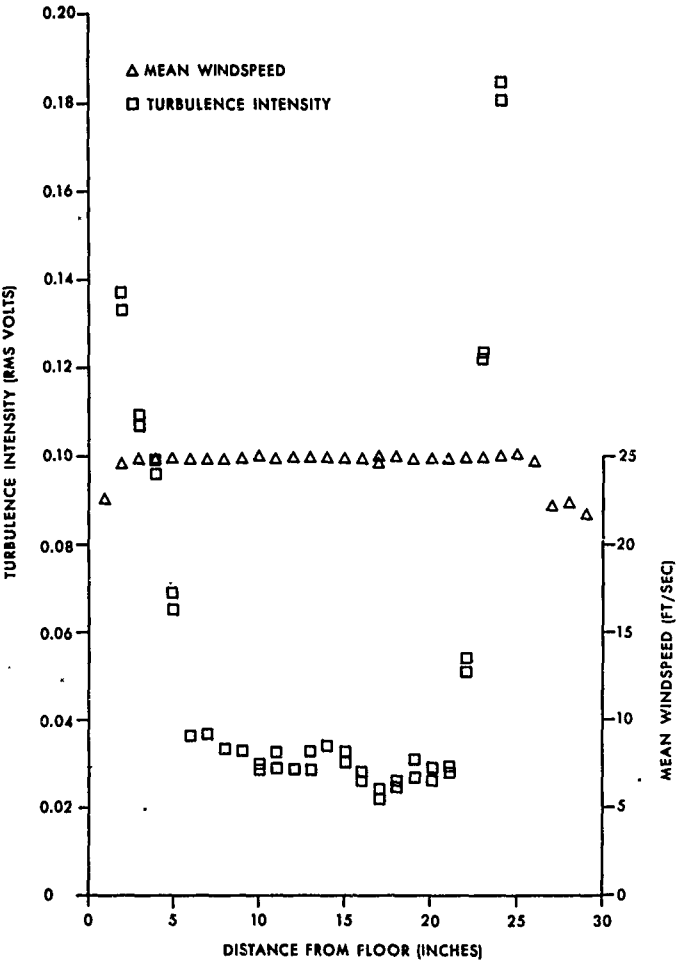

Figure A-27. Vertical Profile of the Longitudinal Velocity at Distance Downstream of 55 Inches With a Leak in the Entrance Filter